arXiv:1210.6759v1 [hep-th] 25 Oct 2012

Holographic Entanglement Entropy of AdS Solitons and Tensor Network States

J. Molina-Vilaplana

Department of Systems Engineering and Automation.
Technical University of Cartagena.
C/Dr Fleming S/N. 30202. Cartagena. Spain[*]

Abstract

The recent proposal connecting the AdS/CFT correspondence and entanglement renormalization tensor network states (MERA) is investigated by showing that the entanglement entropy and the two point functions in a type of hybrid tensor network state composed by a finite number of MERA layers and a matrix product state (MPS) acting as a cap layer, imitate the behaviour of the holographic entanglement entropy and the two point functions in the AdS soliton geometry. Within the context of AdS/CFT, AdS solitons represent theories with a mass gap, i.e gapped systems. From these observations, an explicit connection between the entanglement structure of the tensor network and those parameters which define the AdS soliton geometry is provided.

---

[*] Electronic address: Javi.Molina@upct.es

Contents

I. Introduction 2

II. Tensor Network States for 1-D systems 5

A. Matrix Product States 5

B. Entanglement renormalization tensor network states. MERA 8

C. Hybrid MERA-MPS networks 11

III. The AdS/MERA duality 13

IV. Holographic Entanglement Entropy in AdS Solitons and Hybrid MERA networks 16

A. Gapless limit: the pure AdS $q_1 = q_2 = 0$ 18

B. Non extremal soliton $q_1 = -q_2 = 1$ 19

C. Extremal Soliton $q_1 \geq 1$, $q_2 > 1$ 21

V. Discussion and Concluding Remarks 26

Acknowledgments 27

References 28

I. INTRODUCTION

The best known concrete realization of the holographic principle is the AdS/CFT correspondence [1]. This duality is generally formulated as the equivalence between the generating functionals $\mathcal{Z}$ of two very different theories: a classical theory of supergravity defined on a $D+1$ asymptotically Anti de Sitter spacetime and a QFT living on a D-dimensional spacetime that is the boundary of the AdS, i.e,

$$\mathcal{Z}_{QG}\left[AdS_{D+1},\, \mathcal{J}(x,z)\right] \equiv \mathcal{Z}_{QFT}\left[\partial(AdS)_D,\, J(x)\right] \ , \tag{1}$$

and more explicitly,

$$e^{-S_{QG}[\mathcal{J}(x,z)]} \sim \left\langle e^{-\int J(x)\, \mathcal{O}(x)\, d^D x} \right\rangle_{\mathcal{J}(x,0)\equiv J(x)} \ , \tag{2}$$

where x are the spacetime dimensions of the QFT, z is the extra-dimension of the gravity theory on AdS, $\mathcal{O}$ are operators of the quantum field theory on the boundary, and $\mathcal{J}(x,z)$ are the classical fields of the gravitational theory whose boundary values $\mathcal{J}(x,z)|_{z\to 0}$ act as the sources $J(x)$ for the correlation functions of the QFT.

Since the initial formulations of the correspondence, a huge amount of work has been carried out in order to generalize the AdS/CFT while providing numerous valuable models to study non-perturbative effects in quantum field theory such as confinement and quantum phase transitions. However, still there is not a first principles derivation of the correspondence that allow us to explicitly construct a bulk gravity theory from a boundary QFT [2]. Nevertheless, it is widely accepted that the AdS/CFT is at heart a geometric formulation of the renormalization group (RG), in which the renormalization scale becomes the extra radial dimension z and the beta functions of the boundary field theory are the saddle point equations of motion of the bulk gravity theory [3].

In recent years, ideas coming from quantum information have been especially relevant in establishing new numerical real space quantum renormalization group methods such as density matrix renormalization group (DMRG) [4], and tensor network states (TNS) algorithms including matrix products states (MPS) [5], projected entangled-pair states (PEPS) [6], multi-scale renormalization ansatz (MERA) [9], tensor renormalization group (TRG) [7], and tensor-entanglement-filtering renormalization (TEFR) [8]. These algorithms provide a set of variational *ansatze* useful to characterize the low-energy (long distance) physics of quantum many-body systems. The TNS assumes a parameterization of a many-body wave-function by means of a collection of tensors connected into a network. The number of parameters required to specify these tensors is much smaller than the exponentially large dimension of the system's Hilbert space, allowing for the efficient representation of very large (and even infinite) systems. It has been recently proposed [11] that tensor network states can be broadly classified into two categories according to the geometry of the underlying networks.

In the first category, the network mimics the physical geometry of the system, as specified by the pattern of interactions in the Hamiltonian. The MPS ansatz for one dimensional systems, which consists of a collection of tensors connected into a chain and its generalization for higher dimensional systems (PEPS), lie on this *physical geometry* category.

At variance, according to [11], the collection of tensors in the second category of TNS are connected so as to parametrize the diferent length scales (or, equivalently, energy scales) relevant to the description of the many-body wave-function. These tensor networks organize the quantum information contained in a state in terms of different scales through a characteristic tensor connectivity which spans an *additional* dimension related with the RG scale, as for instance in MERA. This has been used to define a generalized notion of holography inspired by the AdS/CFT duality [10]. There, the author has made the groundbreaking observation that the tensor networks in MERA, happens to be a realization of the AdS/CFT correspondence. In [10], the dual higher dimensional holographic geometry of the original system emerges when one realizes that the tensors in MERA corresponding to a one dimensional quantum critical point, are connected so as to reproduce a discrete version of the anti-de Sitter spacetime (AdS). After the initial proposal, a substantial amount of work has appeared supporting and extending the original idea [11–22].

Within the context of the AdS/CFT correspondence, the holographic dual of a gapped system is the capped holographic geometry called the AdS soliton This capping of the AdS geometry implies an infrared (IR) fixed point at a finite energy scale for the original CFT lying at the boundary of AdS, thus yielding the dual for a massive deformation of the theory. As the AdS soliton is dual to a gapped system, it is expected that the IR state will be a non entangled state if there is no *topological order*. However, it also might be the case of nontrivially entangled IR states in extremal solitons, which could be due to some underlying topological order [16]. In [16], authors speculated, in terms of the AdS/MERA duality, about the structure of a tensor network that might suitably describe this possibility.

The aim of this paper is to offer new insights on the connection between the structure of MERA states and their potential holographic descriptions by exploring some hints posed in [16]. Here we explicitly show that the entanglement entropy and the two point functions in a type of hybrid tensor network state (composed by a finite number of MERA layers and an MPS acting as a cap layer) representing a one dimensional quantum many body system, imitate the behaviour of the holographic entanglement entropy and the two point functions in the capped holographic geometries described by AdS solitons. From these observations, we provide a connection between some parameters of the tensor network representation of the system and those parameters defining the holographic geometry of an AdS soliton.

The paper is organized as follows: In section two, MPS and MERA tensor network states are briefly reviewed and the hybrid tensor network composed of a finite number of

MERA layers and a capping MPS on the top layer is presented. Section three reviews, the AdS/MERA conjecture and its relation with the formula for the computation of holographic entanglement entropy [23]. In section four, the entanglement entropy and the two point functions in AdS soliton geometries are contrasted with those results obtained when computing these quantities in the hybrid tensor network presented in section two. Finally, in section five, results are summarized and future research problems are exposed.

II. TENSOR NETWORK STATES FOR 1-D SYSTEMS

Tensor network states constitute a new class of numerical methods that aim to efficiently describe ground states of strongly correlated quantum systems. TNS implement techniques drawed from renormalization group methods and the knowledge about the structure of entanglement in the ground states of quantum many body systems. In this section we briefly review some issues concerning the two classes of tensor network states (MPS and MERA) used in this paper in order to offer further evidence of the connection between AdS/CFT and MERA.

A. Matrix Product States

Let us first to consider a 1-D translationally invariant quantum many body system composed by N sites of dimension d. Its ground state can be expressed as

$$|\Psi\rangle = \sum_{s_1,s_2,\cdots,s_N=1}^{d} \mathcal{T}_{s_1,s_2,\cdots,s_N} |s_1, s_2, \cdots, s_N\rangle \ , \tag{3}$$

where for $j \in \{1, \cdots, N\}$ and $s_j \in \{1, \cdots, d\}$, the vectors $|s_j\rangle \in \mathcal{H}_d$ form the computational basis of the j-th system site and where the type - $\left(\begin{smallmatrix} 0 \\ N \end{smallmatrix}\right)$ tensor $\mathcal{T}_{s_1,s_2,\cdots,s_N} = \langle s_1, s_2, \cdots, s_N|\Psi\rangle$ represents the associated probability amplitudes. The MPS representation of this state is given by the ansatz [5],

$$\mathcal{T}_{s_1,s_2,\cdots,s_N} = \mathrm{Tr}\ (A^{s_1}\, A^{s_2}\ \cdots A^{s_N}\ )\ , \tag{4}$$

where A^{s_j} are matrices of dimension $\mathcal{M}$ with elements $A^{s_j}_{\alpha,\beta}$ whose values are determined by means of a variational search procedure. Away from the critical point, a finite $\mathcal{M}$ suffices to exactly describe the ground state. Essentially, the so called bond dimension $\mathcal{M}$, controls

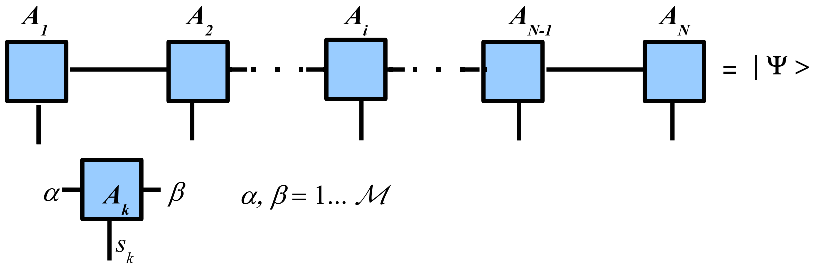

FIG. 1: Pictorial representation of the MPS *ansatz*. The matrices A^{s_k} are three indices tensors (excepting the first A^{s_1} and last A^{s_N} tensors, which only have two indices due to open boundary conditions), with s_k related with the physical site k and α and β as the indices of the correlation space of dimension $\mathcal{M}$ linking to the two neighboring matrices $A^{s_{k-1}}$ and $A^{s_{k+1}}$. In the figure, connecting two adjacent tensors through a given link is equivalent to contracting the product of these two tensors through the corresponding index. Applying this rule to all the matrices of the picture results in equation (4).

how much entanglement between adjacent sites is retained during the variational procedure. Treating the matrices A^{s_j} as $\binom{1}{2}$ tensors (one extra index is due to the physical site), the MPS ansatz can be pictorially described as in figure 1.

Regarding the computation of observables with the MPS ansatz, given the state (3) with coefficients (4), the expectation value of an operator $\Theta = \mathcal{O}_1 \otimes \mathcal{O}_2 \otimes \cdots \otimes \mathcal{O}_N$ which is the tensor product of local operators $\mathcal{O}_j$ for each site j, can be expressed as (Fig.2),

$$\langle \Psi | \Theta | \Psi \rangle = \mathrm{Tr} \left(\mathbb{E}_{\mathcal{O}_1} \mathbb{E}_{\mathcal{O}_2} \cdots \mathbb{E}_{\mathcal{O}_{\mathrm{N}}} \right) \ . \tag{5}$$

The *transfer matrices* $\mathbb{E}_{\mathcal{O}_j}$ are defined by,

$$\mathbb{E}_{\mathcal{O}_j} = \sum_{s_j, s_j^{'}=1}^{d} \langle s_j^{'} | \mathcal{O}_j | s_j \rangle \left(A^{s_j} \otimes \bar{A}^{s_j^{'}} \right) \ , \tag{6}$$

and $\bar{A}^{s_j^{'}}$ is the hermitian conjugate of A^{s_j}. As a result, as posed in equation (5), the computation of expectation values with MPS, may be viewed as the total contraction of a 1-dimensional array of tensors ($\mathbb{E}_j$).

It is well known that an MPS with a finite bond dimension $\mathcal{M}$, faithfully represents the ground state of a 1D gapped system and supports the exponential decay of correlations expected for these models. Considering a translational invariant matrix product state $|\Psi\rangle$,

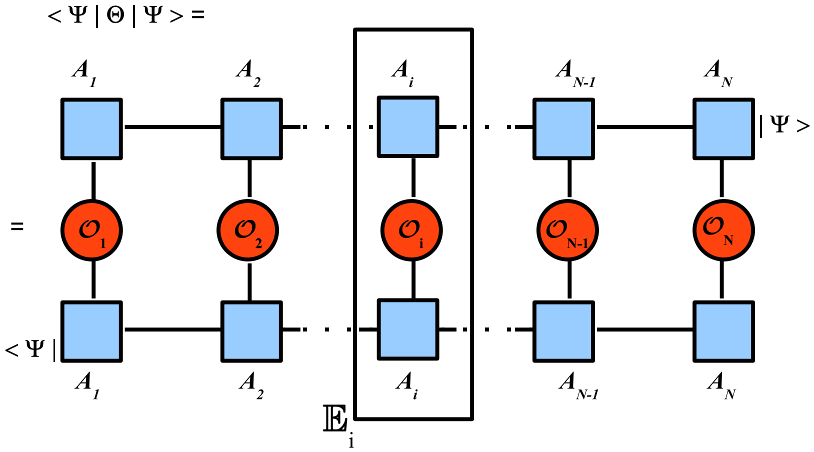

FIG. 2: Pictorial representation of an expectation value computation through the MPS *ansatz* given by equations (5) and (6).

homogeneously defined by the matrices A_s, the two point correlation function of two local observables Θ_α and Θ_β, with support on sites s_i and s_j separated an arbitrary distance $\ell+1$ is defined by,

$$\mathfrak{C}_{\alpha\,\beta}^{[\ell+1]} \equiv \langle\Psi|\Theta_\alpha(s_i)\,\Theta_\beta(s_j)|\Psi\rangle = \mathrm{Tr}\left(\mathbb{E}_{\mathbf{1}}^{[s_1]}\cdots\mathbb{E}_{\Theta_\alpha}^{[s_i]}\cdots\mathbb{E}_{\Theta_\beta}^{[s_j]}\cdots\mathbb{E}_{\mathbf{1}}^{[N]}\right)\ . \tag{7}$$

Following [24], the correlator in the limit when $N\to\infty$ can be written as:

$$\mathfrak{C}_{\alpha\,\beta}^{[\ell+1]} = \sum_{\nu=2}(\lambda_\nu)^\ell\,\mathcal{P}_{\lambda_\nu}^{[\mathbf{B}_\nu]}(\ell)\ , \tag{8}$$

where $\lambda_{\nu\geq 2}$ are the eigenvalues of $\mathbb{E}_{\mathbf{1}}$ for which it holds that $|\lambda_{\nu\geq 2}|<1$, $|\nu\rangle$ and $\langle\nu|$ are the right and left eigenvectors of $\mathbb{E}_{\mathbf{1}}$ for the eigenvalue λ_ν, $\mathcal{P}_{\lambda_\nu}^{[\mathbf{B}_\nu]}(\ell)=\langle\mathbf{1}|\mathbb{E}_{\Theta_\alpha}^{[s_i]}|\nu\rangle\,\langle\nu|\mathbb{E}_{\Theta_\beta}^{[s_j]}|\mathbf{1}\rangle$ are polynomial functions of degree $\mathbf{B}_\nu$ with coefficients depending on λ_ν, and $\mathbf{B}_\nu$ is the size of the largest Jordan block belonging to the generalized eigenspace of λ_ν.

Since every $|\lambda_{\nu\geq 2}|<1$, then the correlator $\mathfrak{C}_{\alpha\,\beta}^{[\ell+1]}$ decay exponentially because it is possible to write its leading behaviour as a superposition of exponentials with decay lengths defined by $\xi_\nu=-1/\log|\lambda_\nu|$. This implies that the MPS gapped nature dominates when probing long range correlations ruled by the eigenvalues λ_ν of the identity transfer matrix $\mathbb{E}_{\mathbf{1}}$.

Furthermore, if one computes the entanglement entropy of a subsystem A within an 1D-MPS state, bipartitioning the system into two subsystems A and B, and then taking the partial trace over the sites on B, it is easy to convince oneself that,

$$S_A \leq 2\,\log\mathcal{M}. \tag{9}$$

Thus, S_A does not scale with the size of the subsystem A despite it can be made arbitrarily large by increasing $\mathcal{M}$. As the entanglement entropy in 1D critical systems scales proportional to $\log \ell$, where ℓ is the size of the subsystem A [39, 40], then, from the bound (9) one clearly sees that an MPS does not support the large amount of entanglement required in quantum critical systems.

B. Entanglement renormalization tensor network states. MERA

The MERA representation of the state 1-D state (3) assumes a decomposition of $\mathcal{T}_{s_1,s_2,\cdots,s_N}$ in terms of a collection of smaller, finite size tensors, which differently from the linear MPS structure, are organized in a two-dimensional layered graph. The sites of the graph represent tensors. They are divided in two groups: the type $\chi - \binom{2}{2}$ tensors with elements $\chi^{u_1,u_2}_{s_1,s_2}$ called *disentanglers* and the type $\Lambda - \binom{1}{2}$ tensors with elements $\Lambda^{u_1}_{s_1,s_2}$ called *isometries* (Fig. 3). For quantum critical systems, a MERA tensor network posses a characteristic scale invariant structure, i.e, a unique χ and a unique Λ precisely define the MERA graph.

The MERA representation of (3) implements an efficient real space renormalization group procedure through a tensor network organized in different layers labelled by τ. Each layer of MERA defines a RG transformation: prior to the renormalization of a block of typically two sites located at layer τ into a single site by means of a Λ^{τ}-type tensor, short range entanglement between the sites is removed by means of the *disentangler* χ^{τ}. In other words, the MERA tensor networks, as a consequence of the locality of physical interactions in the ground state of many-body systems, at each layer, decouple the relevant low energy degrees of freedom from the high energy ones, which are then safely removed, by unitarily transforming with *disentanglers* small regions of space. The MERA coarse-graining transformation induces an RG map that can be applied arbitrarily many times keeping constant the computational cost for obtaining consecutive effective theories for the original system which are also labelled by τ.

In a 1D MERA the computation of an observable Θ requires the contraction of a 2D tensor network, and this may be efficiently done by the isometricity requirements for χ and Λ tensors (see figure 4). Indeed, in an scale invariant MERA, contracting an entire layer of

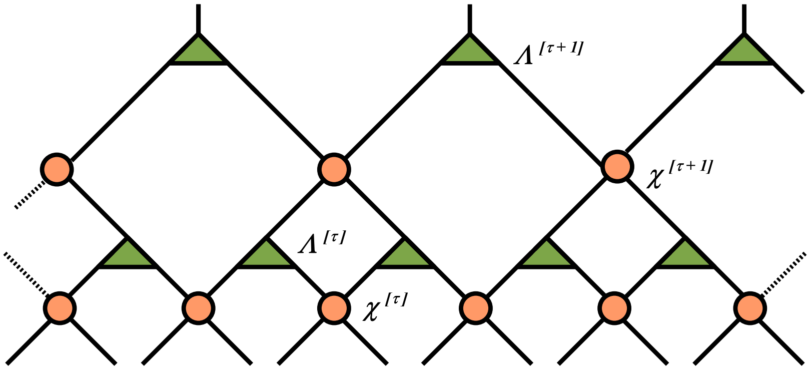

FIG. 3: Pictorial representation of two layers (τ and $\tau+1$) of an scale invariant MERA tensor network. Three legged triangles represent isometries Λ and four-legged circles represent disentanglers χ. At each layer τ, the tensors are chosen so as to fulfill $\chi^{\dagger}\,\chi = \mathbb{I}$ and $\Lambda^{\dagger}\,\Lambda = \mathbb{I}$.

MERA and its conjugate, maps the original expectation value problem into a new one i.e,

$$\langle\Psi|\Theta|\Psi\rangle = \langle\Psi^{'}|\mathcal{S}\,(\Theta)\,|\Psi^{'}\rangle = \langle\Psi^{'}|\Theta^{[1]}|\Psi^{'}\rangle \ , \tag{10}$$

where the quantum state $|\Psi^{'}\rangle$ is the original MERA state $|\Psi\rangle$ after the full contraction of the tensors at the bottom layer with their conjugates, the observable $\Theta^{[1]} = \mathcal{S}\,(\Theta)$ is the *effective* tensor shown inside the rectangle in figure 4 (right), and $\mathcal{S}$ is the *scaling superoperator* [41] of the observable Θ. The total contraction of the tensor network proceeds by mapping the effective observable in a sequential way as,

$$\Theta^{[\tau]} \rightarrow \Theta^{[\tau+1]} = \mathcal{S}(\Theta^{[\tau]}) \ , \tag{11}$$

until the top of the tensor network $|\mathcal{C}\rangle$ is reached, for which it holds that $\langle\Psi|\Theta|\Psi\rangle = \langle\mathcal{C}|\Theta^{[h]}|\mathcal{C}\rangle$, with $h = \log_2 N$ and N being the total size of the system.

One of the most salient features of an scale invariant MERA tensor network is that it naturally supports the well known power-law decaying of correlation functions in systems at the quantum critical point [26]. To show this, it is convenient to define the fixed point *one site scaling superoperator* $\mathcal{S} \equiv \mathcal{S}_{(1)}$ as,

$$\mathcal{S}_{(1)}(\circ) = \sum_{\alpha} \mu_\alpha\, \Phi_\alpha\, \mathrm{Tr}(\Phi_\alpha\, \circ) \ , \tag{12}$$

where the scaling dimensions of the scaling operators Φ_α of the theory are $\Delta_\alpha \equiv -\log_2 \mu_\alpha$ and $\mathrm{Tr}(\Phi_\alpha\, \Phi_\beta) = \delta_{\alpha\beta}$. Let us consider the correlator of two scaling operators $\Phi_\alpha(s_i)$ and

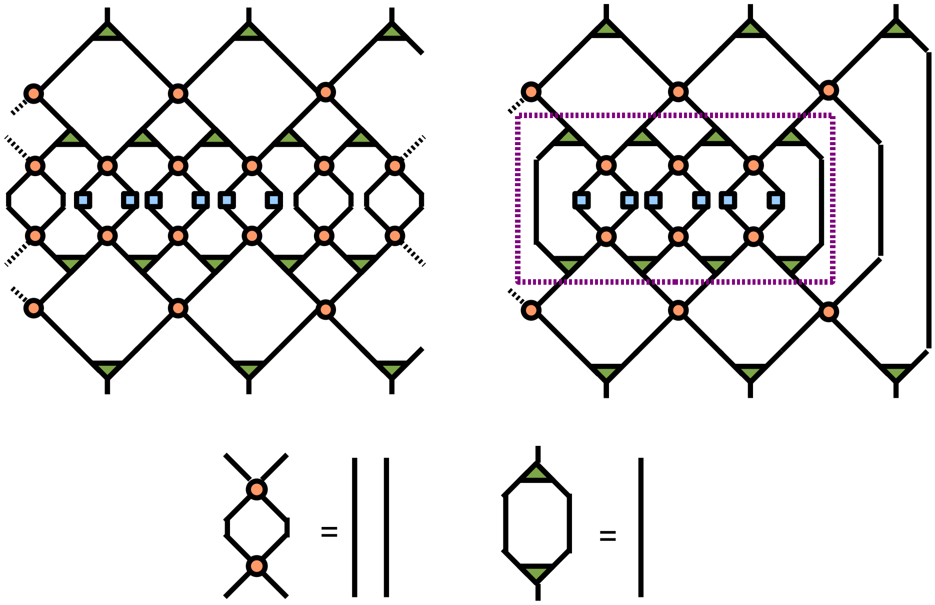

FIG. 4: To compute the expectation value of an observable Θ (blue squares) supportted on an interval of sites, $\{s_1..s_k\}$ with a 1D MERA state, the first layer of disentanglers $\chi^{[1]}$, for which, by definition, holds $\chi^\dagger\chi = \mathbb{I}$ is initially considered. Those $\chi^{u_1,u_2}_{r_1\,r_2}$ whose (both) physical indices do not belong to the support interval $\{s_1..s_k\}$, are trivially contracted with their adjoints. However, this contraction is not trivial for those disentanglers directly connected to the support. The same argument holds for the isometries Λ belonging to the first layer of the MERA state.

$\Phi_\beta(s_j)$ initially located at sites s_i and s_j of the original lattice,

$$\mathfrak{C}_{\alpha\beta} = \langle\Psi|\Phi_\alpha(s_i)\,\Phi_\beta(s_j)|\Psi\rangle\ . \tag{13}$$

After $\tau^* = \log_2|s_i - s_j|$ contractions of the type described above, the sites supporting the original Φ_α and Φ_β become first neighbors [26] and each iteration contributes a factor $\mu_\alpha\,\mu_\beta$ giving,

$$\begin{aligned} \langle\Psi|\Phi_\alpha(s_i)\,\Phi_\beta(s_j)|\Psi\rangle &= \\ = \langle\mathcal{C}^*|\left(\mathcal{S}_{(1)}(\Phi_\alpha(s_i))\right)^\tau\left(\mathcal{S}_{(1)}(\Phi_\beta(s_j))\right)^\tau|\mathcal{C}^*\rangle &= \\ = (\mu_\alpha\mu_\beta)^\tau\langle\mathcal{C}^*|\Phi_\alpha(0)\,\Phi_\beta(1)|\mathcal{C}^*\rangle\ , \end{aligned} \tag{14}$$

where the state $|\mathcal{C}^*\rangle$ is the result of τ^* contractions of the original MERA state with its conjugate. Defining $\mathfrak{C}^{\tau^*}_{\alpha\beta} \equiv \langle\mathcal{C}^*|\Phi_\alpha(0)\,\Phi_\beta(1)|\mathcal{C}^*\rangle$, noticing that $\Delta_{\alpha,\beta} \equiv -\log_2\mu_{\alpha,\beta}$ and recalling the identity $a^{\log b} = b^{\log a}$, the two point function (13) can be written as,

$$\langle \Phi_\alpha(s_i)\, \Phi_\beta(s_j) \rangle = \frac{\mathfrak{C}^{\tau^*}_{\alpha\beta}}{|s_i - s_j|^\eta} \ , \tag{15}$$

with $\eta = (\Delta_\alpha + \Delta_\beta)\delta_{\alpha\beta} = 2\Delta_\alpha$.

C. Hybrid MERA-MPS networks

When considering the ground state $|\Psi\rangle$ of gapped 1D-Hamiltonian $\mathcal{H}$, the correlations decay exponentially at large distances due to the characteristic correlation length ξ, while typically keep power-law decaying for distances smaller than ξ. To emulate this behavior with a tensor network state, it is necessary to have an ansatz which suitably reproduces these features. A potential candidate for this, is a tensor network state with an MPS at the top of a finite number ($\tau_0 \sim \log \xi$) of MERA layers [11]. Here it is assumed that these τ_0 layers correspond to those in the scale invariant MERA describing a neighbouring critical point while the capping MPS accurately describes the behaviour of the long distance correlations in the gapped phase.

In the MERA representation of the ground state of a gapped Hamiltonian, after $\tau_0 \approx \log \xi$ renormalization steps, the original ground state $|\Psi_0\rangle$ of the system has flowed into a state $|\Omega\rangle$ that can be well approximated by a product state with no entanglement between the different coarse grained lattice sites. This state describes the ground state at a fixed-point of the RG flow corresponding to a gapped phase without topological order. Nevertheless, the finite layered MERA may also be combined with another tensor network (an MPS in figure 5) in order to represent the ground states of gapped systems that flow towards non trivially entangled IR fixed point ground states $|\Phi\rangle$.

The MPS tensor at the top layer of this hybrid MPS-MERA state, accounts for the gapped character and non trivial long range entanglement of the IR fixed point in a natural way, i.e, it naturally arranges the exponential decay of the two point correlations at distances larger than ξ, while the MERA '*curtain*' of τ_0 layers implements the power-law decaying behaviour of correlators when the distance between the physical sites is smaller than ξ. The case of the trivial non-entangled product IR state $|\Omega\rangle$ is represented by an MPS with bond dimension $\mathcal{M} = 1$.

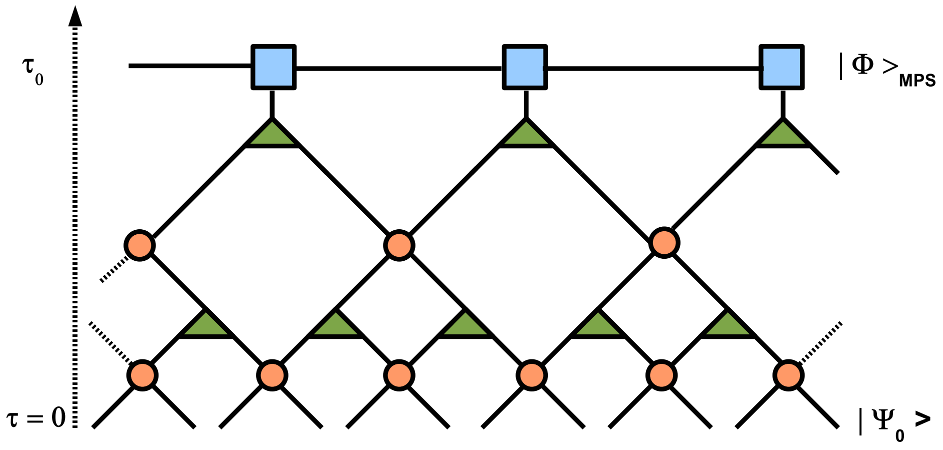

FIG. 5: Pictorial description of an Hybrid MPS-MERA tensor network state with a fixed number τ_0 of MERA layers and a top tensor given by an MPS. The original ground state of the system $|\Psi_0\rangle$ lies at the first layer of the MERA *curtain* while the ground state at the IR fixed point is given by the MPS tensor capping the MERA geometry.

In the MPS-MERA tensor network, the total system size N is given by,

$$N = 2^{\tau_0}\, m \ , \tag{16}$$

where m, is the number of *effective* MPS sites located at the top of the τ_0-th layer of the binary MERA '*curtain*' hanging from the MPS tensor. Regarding the entanglement that may be supported by these type of tensor states, as each "site" in the top MPS represents a cluster of $\sim 2^{\tau_0}$ coarse grained sites of the original lattice, then the entanglement between different sites of this tensor represents the long range entanglement between distant clusters of sites in the original system. As a result, if the MPS cap tensor is not the trivial product state, its long-range entanglement, which relates with some type of topological order, will have a non zero contribution to the total entanglement entropy of a region A in the original lattice. As an example, the ground states of 1D systems in the Haldane phase, show a kind of symmetry protected topological order [27]. In the tensor network representation of a system with this type of topological order, the local unitary transformations carried out by the disentanglers of the MERA "*curtain*" only remove the short range entanglement, i.e., the entanglement between the neighboring sites. At variance, the long range entanglement (i.e, the entanglement between distant sites), is not removed by disentanglers. It is precisely this robustness of the long range entanglement under local operations which entails the non trivial topological order of the IR fixed point state represented by the MPS at the top of the MERA *curtain*.

III. THE AdS/MERA DUALITY

In [10], it was firstly observed that MERA [9] happens to be a realization of the AdS/CFT correspondence [1]. As pointed out in [10], from the entanglement structure of a quantum critical many body system, is possible to define a higher dimensional geometry in which, apart from the coordinates labelling the position and the time t, one may add a "radial" coordinate z labelling the hierarchy of scales. Then, the higher dimensional geometry emerging from MERA may be visualized by locating cells around all the sites of the tensor network representing the quantum state. The size of each cell is defined to be proportional to the entanglement entropy of the site in the cell. Through this procedure, a geometric dual picture of the tensor network arises quite naturally from the entanglement of the degrees of freedom of the critical system lying on the boundary [12, 20].

The discrete geometry emerging at the critical point is a discrete version of AdS. For a one-dimensional quantum critical system with a space coordinate labelled by x, the continuous isometry $w \to w + \theta$, $x \to e^{\theta} x$ of the metric

$$ds^2_{\mathrm{AdS}} \sim dw^2 + e^{-2w} \left(dx^2 - dt^2\right) \ , \tag{17}$$

is replaced by the MERA's discretized version, $w \to w+k$, $x \to 2^k x$ or $x \to 3^k x$ depending on the binary or ternary implementation of the renormalization algorithm [9]. Here, the extra direction w in the AdS is identified with τ (the variable labelling the number of renormalization steps) in MERA. To be more concrete, the $(D+1)$-dimensional AdS metric can be written in the form,

$$ds^2_{\mathrm{AdS}} = \frac{L^2_{\mathrm{AdS}}}{z^2} \left(dz^2 - dt^2 + dx^2\right) \ , \tag{18}$$

where, L_{AdS} is a constant called the AdS radius; it has the dimension of a length and it is related with the curvature of the AdS space. We have also made the change of variable $\tau = \log z$, where z is the standard radial coordinate of the Poincaré AdS. With this choice of the spacetime coordinates, the one dimensional quantum critical system lies at the boundary $(z = 0)$ of the bulk geometry.

The most convenient way to establish the AdS/MERA connection is to compare the procedures to compute the entanglement entropy in both cases. In the classical gravity limit of AdS/CFT, Ryu and Takayanagi (RT) derived a celebrated formula yielding the entanglement entropy of a region A provided that the (boundary) conformal field theory describing the critical system admits an holographic gravity dual [23]. In the RT approach, the entanglement entropy is obtained from the computation of a minimal surface in the dual higher dimensional gravitational geometry (bulk theory); as a result, the entanglement entropy S_A in a CFT_D is given by the area law relation,

$$S_A = \frac{\mathrm{Area}(\gamma_A)}{4G_N^{(D+1)}} \ , \tag{19}$$

where D is the number of spacetime dimensions of the boundary CFT, γ_A is the D-dimensional static minimal surface in AdS_{D+1} whose area is given by $\mathrm{Area}(\gamma_A)$ and $G_N^{(D+1)}$ is the $D+1$ dimensional Newton constant. In the RT proposal, looking for the minimal surface γ_A separating the degrees of freedom contained in region A from those contained in the complementary region B, amounts to search for the severest entropy bound on the information hidden in the AdS_{D+1} region related with B. Despite the RT formula has not been rigorously proven its validity is supported by very reassuring evidence [23, 28, 29].

In this paper, the interest will be mainly focused in the $D = 2 = (1+1)$ case, for which the equation (19) reduces to,

$$S_A = \frac{\mathrm{Length}(\gamma_A)}{4G_N^{(3)}} \ . \tag{20}$$

Namely, there is a striking similarity between the formula (20) and the computation of the entanglement entropy of a region A with MERA. Using MERA, the entanglement entropy is fixed by the structure of the *causal cone* [9, 25]. The causal cone $\mathcal{CC}(A)$ of a region A of ℓ sites, is determined by all the disentanglers and isometries along all the levels of the tensor network, which are directly connected with the sites in the original region A, (see figure 6). As a result, to compute the entropy S_A it is necessary to trace out any site within the tensor network which does not lie in $\mathcal{CC}(A)$. The boundary of the $\mathcal{CC}(A)$ is a curve $\widetilde{\gamma}_A$. The length of $\widetilde{\gamma}_A$ is, when multiplied by the maximal contribution to entanglement entropy given by each traced out site, the sum of the entropies of all the traced out sites [9, 10], and thus provides an upper bound for the entropy S_A [11],

$$S_A \leq \mathrm{Length}(\widetilde{\gamma}_A)\, \log W \ , \tag{21}$$

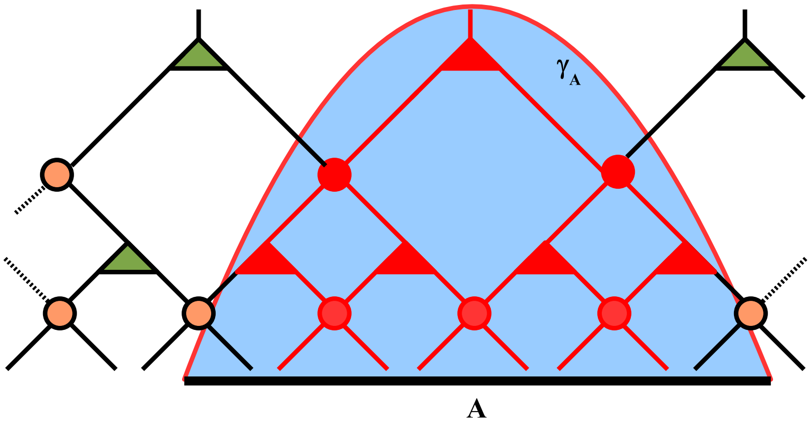

FIG. 6: The causal cone of a block of sites in MERA (in red) is given by the minimal number of tensors that may affect to the expectation value of any observable with support on those sites. The boundary of the causal cone of an interval A defines a curve $\widetilde{\gamma}_A$ which length, in an optimized MERA, acts as the bound for the entanglement entropy of the region A given in equation (21).

where W is the dimension of the auxiliary space of disentanglers and isometries. For instance, for disentanglers $\chi^{u_1\,u_2}_{v_1\,v_2}$, $u_{1,\,2} \in \{1, \cdots, W\}$ and $v_{1,\,2} \in \{1, \cdots, W\}$.

The close connection with the RT formula emerges as one realizes that $\widetilde{\gamma}_A$ can be regarded as the minimal curve γ_A in the RT proposal, since it counts the minimal number of sites which must be traced out in the MERA tensor network. Indeed, the minimal curve $\widetilde{\gamma}_A$ in an optimized scale invariant MERA network [11] saturates the bound given in (21); this has been confirmed by explicit computation in one dimensional critical systems, where it has been shown that [9],

$$S_A \sim k \cdot \log \ell. \tag{22}$$

where k is a constant of order one. Since $\widetilde{\gamma}_A$ is defined as the boundary of the $\mathcal{CC}(A)$, it can be interpreted as an holographic screen which optimally separates the region in the MERA tensor network related with the degrees of freedom of A, from those in its complementary region B.

Despite a complete characterization of the AdS/MERA duality is still lacking, very recent advances point to fulfill this objective. In [20], authors have used a continuos version of MERA (cMERA, [21]), the holographic formula for the entanglement entropy and the concept of distance between quantum states to address one of the major issues concerning the AdS/MERA conjecture, i.e, how gravity duals arise from the structure of the quantum entanglement of the quantum critical systems under consideration. The question about the role of the large N limit in the AdS/MERA duality is also considered in [20] as well as in [22], where it is shown how a number of features of the holographic duality in the large N limit emerge naturally from entanglement renormalization tensor networks.

IV. HOLOGRAPHIC ENTANGLEMENT ENTROPY IN AdS SOLITONS AND HYBRID MERA NETWORKS

It is widely accepted that, non-local observables such as two-point functions, entanglement entropy and Wilson loops turn out to be crucial for elucidating the subtleties of the AdS/CFT correspondence [1]. In this section, the holographic entanglement entropy and general features of two point correlators in AdS soliton geometries are calculated while interpreting the results in the light of those obtained when computing these quantities by means of the hybrid MERA tensor network described in section II C.

Within the context of the AdS/CFT correspondence, the holographic dual of a gapped system is the AdS soliton, obtained by double Wick rotating the AdS black hole and then compactifying one of the spatial dimensions transverse to the AdS radial dimension. The compact dimension shrinks to zero at some finite value z_0 of the AdS radial coordinate, capping the AdS geometry. The radial coordinate together with the shrinking of the compact dimension make a type of cigar geometry, with the IR end of space corresponding to the tip of the cigar. Furthermore, this capping of the AdS geometry implies an IR fixed point at a finite energy scale ($\sim 1/z_0$) for the CFT lying at the boundary of AdS, thus yielding the dual for a gapped massive system.

Here it will be considered the AdS$_3$ soliton metric, which in Poincaré coordinates is given by,

$$ds^2_{\mathrm{Sol}} = \frac{L^2_{AdS}}{z^2}\left[\frac{dz^2}{f(z)} + f(z)\,dx^2 - dt^2\right] \ , \tag{23}$$

with L_{AdS} as the AdS characteristic length and the function $f(z)$,

$$f(z) = \left(1 - q_1\,\frac{z}{z_0}\right)\left(1 - q_2\,\frac{z}{z_0}\right) \ , \tag{24}$$

for which it holds that $f(z_0) = 0$. In this coordinate system, the boundary is the $z = 0$ slice and the geometry is capped off at $z = z_0$ while keeping asymptotically AdS since

$f(z) \to 1$ as $z \to 0$. As it will be shown, different values of the parameters q_1 and q_2 give rise to different IR behaviours for the holographic entanglement entropy and the two point functions. In this sense, the pure AdS space can be obtained by simply choosing $q_1 = q_2 = 0$ in (24) while the simplest capped geometry, the non extremal soliton is defined by choosing $q_1 = -q_2 = 1$ in (24), which results in $f(z) = 1 - \left(\frac{z}{z_0}\right)^2$.

In order to obtain the entanglement entropy of an static region A lying at the boundary of an asymptotically AdS spacetime, the Ryu and Takayanagi proposal [23] accomplishes the task throgh the computation of an static surface of minimal area in the bulk geometry. In AdS$_3$, this means a static curve of minimal length γ, i.e a geodesic. The metric (23) on the fixed time slice is given by,

$$ds^2_{\text{Sol}}|_{t=0} = \frac{L^2_{AdS}}{z^2}\left[\frac{dz^2}{f(z)} + f(z)\,dx^2\right] . \tag{25}$$

Let us now consider the region A in the boundary given by an interval with length ℓ along x direction. Choosing the origin in the center of this interval, the symmetry of the problem allows us to restrict to curves described by an even function $z = z(x)$. Then, the length functional that we have to minimize to compute the holographic entanglement entropy reads,

$$\text{Length}(\gamma) = 2\int_{z_m}^{\epsilon} \frac{L_{AdS}}{z}\,dx\,\sqrt{\frac{\dot{z}^2}{f(z)} + f(z)}\ , \tag{26}$$

where $\dot{z} = dz/dx$ and z_m satisfies that $z(0) = z_m$ while $z(\ell/2) = \epsilon$ (see figure 7). Considering the integrand of (25) as a Lagrangian density $\mathcal{L}[\dot{z}, z]$, one notices that it does not depend explicitly on x. Namely, the independence of $\mathcal{L}[\dot{z}, z]$ on x leads to the conserved quantity $\mathcal{H} = p_z\,\dot{z} - \mathcal{L}$, where $p_z = \partial\mathcal{L}/\partial\dot{z}$. In particular, one gets $\mathcal{H} = -(f(z)/z)\,(\dot{z}^2/f(z) + f(z))^{-1/2}$. The constancy of $\mathcal{H}$ can be expressed by settling that $z_m = 1/\mathcal{H}$ which allows to write,

$$\dot{z} = -\frac{f(z)}{z}\sqrt{z_m^2 f(z) - z^2}\ , \tag{27}$$

as one notices that $\dot{z} < 0$. Replacing (27) in (26), the geodesic length used in the formula for the computation of the holographic entanglement entropy (20), acquires the form,

$$\text{Length}(\gamma) = -2L_{AdS}\int_{z_m}^{\epsilon} \frac{z_m\,dz}{z\sqrt{z_m^2\,f(z) - z^2}}\ . \tag{28}$$

In addition, the two point functions of scaling operators Φ inserted at two spacelike separated points on the boundary of AdS are also considered. According to [1], this correlator

$\mathfrak{C}_{\Phi}^{[\mathcal{D}]}$, is obtained from the spacetime propagator $\mathfrak{C}_{\text{Holo}}^{[\mathcal{D}]}$ between the corresponding points on the UV-cutoff boundary lying at $z \sim \epsilon$ by simply writting,

$$\mathfrak{C}_{\Phi}^{[\mathcal{D}]} = \epsilon^{-2\Delta}\, \mathfrak{C}_{\text{Holo}}^{[\mathcal{D}]} \,, \tag{29}$$

where $\mathcal{D}$ is the distance between the inserted operators on the boundary and Δ is the scaling dimension of the operator Φ. The holographic propagator $\mathfrak{C}_{\text{Holo}}^{[\mathcal{D}]}$, in the leading order of its semi-classical approximation, is given by a sum over geodesics $\Upsilon_{\mathcal{D}}$ connecting the points on the cut-off boundary,

$$\mathfrak{C}_{\text{Holo}}^{[\mathcal{D}]} = \sum_{\Upsilon_{\mathcal{D}}} e^{-m\,\text{Length}(\Upsilon_{\mathcal{D}})} \sim e^{-m\,\text{Length}(\gamma_{\mathcal{D}})} \;. \tag{30}$$

Here, $\text{Length}(\gamma_{\mathcal{D}})$ is the length of the shortest geodesic connecting the two boundary points and m is the mass of the fields ϕ dual to the scaling operatots Φ. In the AdS/CFT correspondence, the scaling dimensions of operators inserted at the boundary CFT are related to the masses m of their dual fiels in the bulk geometry. For instance, when Φ is an scalar operator of large scaling dimension Δ, then it holds that $\Delta \approx m\, L_{AdS}$ [1].

A. Gapless limit: the pure AdS $q_1 = q_2 = 0$

The pure AdS space is obtained by choosing $q_1 = q_2 = 0$ in equation (24), i.e, $f(z) = 1$. For convenience from here in advance, we simply write $L_{AdS} = L$. Replacing $f(z) = 1$ into (28) and carrying out the integration one obtains,

$$\text{Length}(\gamma) = 2L\left[\log\frac{z_m + \sqrt{z_m^2 - z^2}}{z}\right]_{z_m}^{\epsilon} = 2L\,\log\frac{2\,z_m}{\epsilon} \;. \tag{31}$$

As a result, the holographic entanglement entropy of a region A of length ℓ reads (as one realizes that $\ell = 2\,z_m$, see figure 7 upper part left),

$$S_A = \frac{\text{Length}(\gamma)}{4G_N^{(3)}} = \frac{c}{6\,L}\,2L\,\log\frac{2z_m}{\epsilon} = \frac{c}{3}\,\log\frac{\ell}{\epsilon} \;. \tag{32}$$

Here, it has been used the celebrated relation between $L/G_N^{(3)}$ and the central charge c of the boundary CFT given in [30],

$$c = \frac{3\,L}{2\,G_N^{(3)}} \;. \tag{33}$$

The equation (31) also allows to compute the two point function of an scaling operator Φ of large scaling dimension Δ inserted at two points separated by a distance $\mathcal{D} \equiv \ell$. Making use of the equations (29) and (30), this correlator amounts to,

$$\begin{aligned} \mathfrak{C}_{\Phi}^{[\ell]} &= \epsilon^{-2\Delta}\, e^{-m\,\mathrm{Length}(\gamma)} = \\ &= \epsilon^{-2\Delta}\, e^{-m\,2L\log \ell/\epsilon} \approx \\ &\approx \epsilon^{-2\Delta}\, e^{-2\Delta\,\log \ell/\epsilon} = \ell^{-2\Delta} \ , \end{aligned} \tag{34}$$

which is exactly the power-law decaying of the correlation functions expected for the ground state of a critical system which geometric dual is given by the pure AdS space. It is clear since [10] and the exposition above that, the behaviour of two point functions and entanglement entropy in pure AdS space are well represented in terms of an scale invariant MERA tensor network (see equations (15) and (22) in sections II B and III respectively).

B. Non extremal soliton $q_1 = -q_2 = 1$

The simplest AdS soliton is the non extremal soliton, obtained by taking $q_1 = -q_2 = 1$ in equation (24). In this case, the function $f(z)$ reads as,

$$f(z) = \frac{1}{z_0^2}\left(z_0^2 - z^2\right) \ . \tag{35}$$

The computation of the geodesic length (28) for this geometry yields,

$$\mathrm{Length}(\gamma) = 2L\left[\log\frac{a + \sqrt{a^2 - z^2}}{z}\right]_{z_m}^{\epsilon} \ , \tag{36}$$

where $a^2 = \frac{z_m^2\, z_0^2}{z_m^2 + z_0^2}$. In the limit $z_m \ll z_0$, $a \sim z_m$ and (36) reduces to (31). However, here we are interested in probing the entanglement entropy in the IR regions of the geometry [16, 31, 32], i.e, when $z_m \gg z_0$ and $a \sim z_0$. In this limit, and requiring that the integral have a real value, the geodesic length amounts to,

$$\mathrm{Length}(\gamma) = 2L\left[\log\frac{z_0 + \sqrt{z_0^2 - z^2}}{z}\right]_{z_0}^{\epsilon} = 2L\,\log\frac{2z_0}{\epsilon} \ . \tag{37}$$

As a result, one finds a saturated length of γ when probing the IR geometry of the non extremal soliton, which through (20), translates into the well known saturation for the entanglement entropy in gapped phases [23, 33],

$$S_A = S_0 \sim \log\frac{2z_0}{\epsilon} \ . \tag{38}$$

In other words, in the non extremal soliton geometry, the entanglement entropy which corresponds to small ℓ is similar to (32) and the geodesic has a turning point at z_m. At variance, when the minimal curve probes the region $z \sim z_0$, its length saturates yielding the well known saturation of the entanglement entropy in gapped phases. Namely, when $\ell \gg z_0$, the minimal curve γ, after having probed all the length scales smaller than z_0, finishes at two endpoints located at $z = z_0$ (see figure 7, lower part, right) and the longest *complete* geodesic curve able to connect two boundary points is the γ curve between two points separated at a distance $\mathcal{D} = 2\, z_0$ with the turning point at $z_m = z_0$. When $\mathcal{D} > 2\, z_0$, there are no geodesic curves directly connecting the boundary points, a signature of the vanishing of the two point functions for distances larger than $2\, z_0$.

The entangling nature of the IR fixed point exposed by the large ℓ expansion of the minimal curve γ, can be interpreted in terms of the hybrid MPS-MERA tensor network states described in section II C. With this aim, a tensor network composed of a MERA *curtain* of $\tau_0 = \log \xi$ layers, with $\xi = 2\, z_0$ is considered. On the top of the *curtain*, there is an MPS state $|\Omega\rangle$ with bond dimension $\mathcal{M} = 1$ which corresponds to the trivial non entangled product state,

$$|\Omega\rangle = |0\rangle\, |0\rangle \cdots |0\rangle \ . \tag{39}$$

Let us first to compute the entanglement entropy of a region A with $\ell \gg \xi$. In the MERA *curtain*, the causal cone of the region A is connected to the rest of the MERA sites through a number of traced out bonds that is proportional to $\log \xi$ which is independent of ℓ, i.e, $\text{Length}(\widetilde{\gamma}_A) \approx \log \xi$. Using equation (21) one finds that the contribution to entanglement entropy given by the MERA *curtain* is, $S_A^{MERA} \propto \log \xi \sim S_0$ that exactly matches the scaling of the entanglement entropy for the AdS non extremal soliton (38). On the other hand, the product state $|\Omega\rangle$ at the top of the network does not collect any contribution to the entanglement entropy of the region A since these contributions would be bounded by $\log \mathcal{M} = \log 1 = 0$ (see eq.(9)). As a result, the finishing of the geodesic curves γ at two endpoints in z_0 in the non extremal soliton, may be interpreted in terms of an MPS at the top of the MERA *curtain* which results to be the non entangled product state $|\Omega\rangle$.

Next thing to consider is the correlation function of two scaling operators $\Phi(-\ell/2)$ and $\Phi(\ell/2)$ located at the bottom of the MERA *curtain*, $\mathfrak{C}^{\ell}_{\text{TNS}} = \langle \Psi | \Phi(-\ell/2)\, \Phi(\ell/2) | \Psi \rangle$. After

$\tau_0 = \log\xi$ MERA contractions such as those described in section II B one obtains,

$$\begin{aligned} &\langle\Psi|\Phi(-\ell/2)\,\Phi(\ell/2)|\Psi\rangle = \\ &= \langle\Omega|\left(\mathcal{S}(\Phi(-\ell/2))^{\tau_0}\left(\mathcal{S}(\Phi(\ell/2))^{\tau_0}|\Omega\rangle = \right.\right. \\ &= (\mu)^{2\tau_0}\langle\Omega|\Phi(-\ell/2\xi)\,\Phi(\ell/2\xi)|\Omega\rangle\ , \end{aligned} \tag{40}$$

where $|\Psi\rangle$ is the tensor decomposition of the system given by the hybrid MERA-MPS network. Noticing that $\Delta \equiv -\log\mu$, and (8), the correlator can be written as,

$$\begin{aligned} &\langle\Psi|\Phi(-\ell/2)\,\Phi(\ell/2)|\Psi\rangle = \\ &= \xi^{-2\Delta}\,\langle\Omega|\Phi(-\ell/2\xi)\,\Phi(\ell/2\xi)|\Omega\rangle = \\ &= \xi^{-2\Delta}\sum_{|\lambda_\nu|<1} c_\nu\,(\lambda_\nu)^{\ell/\xi} = 0\ , \end{aligned} \tag{41}$$

where in the last equality, it has been used that for the product state $|\Omega\rangle$, $\lambda_\nu \equiv 0$, $\forall$ $|\lambda_\nu| < 1$. This implies that all the two point functions vanish for distances between the boundary points $\mathcal{D} \gg \xi = 2\,z_0$ which completely agrees with the geometric prediction using the AdS/CFT. Finally, it is worth to note here that the conformal behaviour obtained in section IV A is trivially recovered by the hybrid MERA-MPS tensor network when the size of region A is such that $\ell \ll \xi$.

C. Extremal Soliton $q_1 \geq 1$, $q_2 > 1$

The extremal soliton geometry is defined by the class of harmonic functions

$$f(z) = 1 - \alpha\left(\frac{z}{z_0}\right) + \beta\left(\frac{z}{z_0}\right)^2\ , \tag{42}$$

where $\alpha = (q_1 + q_2)$ and $\beta = q_1 q_2$. The geodesic length (28) in the AdS soliton geometry which corresponds to (42) reads as,

$$\begin{aligned} \text{Length}(\gamma) &= -2L\,z_0\int_{z_m}^{\epsilon}\frac{dz}{z\sqrt{z_0^2 - \alpha z_0 z + \varrho z^2}} = \\ &= 2L\,\log\left[\frac{2z_0 - \alpha z + 2\sqrt{z_0^2 + \varrho z^2 - \alpha z_o z}}{z}\right]_{z_m}^{\epsilon}\ , \end{aligned} \tag{43}$$

with $\varrho = \beta - \left(\frac{z_0}{z_m}\right)^2$. In terms of the holographic prescription to compute the entanglement entropy (20), the hints of hidden topological orders encoded in the features of the long range

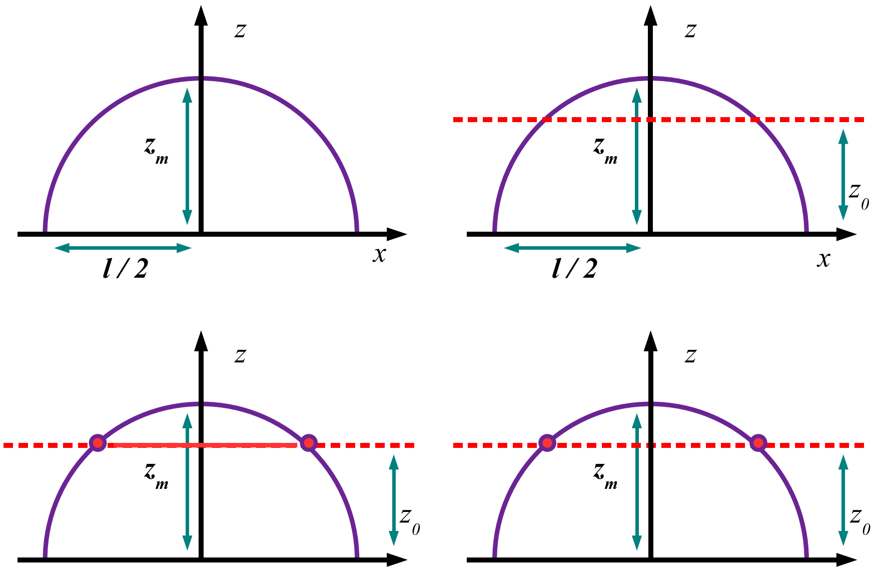

FIG. 7: Geodesics in AdS solitons. Upper half left: In Poincaré coordinates, the geodesics connecting two boundary points separated by distance ℓ in the pure AdS$_3$ spacetime are given by half circumferences with radius $z_m = \ell/2$. Upper half right: An AdS soliton geometry is caracterized by a function $f(z)$ that vanishes at a certain value z_0 of the radial coordinate z. This amounts to say that the holographic geometry given by equation (23) ends at z_0 (discontinuous red line) so geodesics can no longer probe regions with $z > z_0$. Lower half right: the geodesics in the non extremal soliton geometry end at two points lying at $z = z_0$ and Length$(\gamma) \sim \log 2\, z_0$. Lower half left: the geodesics in the extremal soliton geometry, once ariving at $z \sim z_0$, instead of finishing, bend-over the tip of the soliton geometry (red continuous line between points at $z \sim z_0$) giving additional contributions to the geodesic length.

entanglement, should be tracked down at the IR behaviour (the large ℓ expansion) of the UV-independent piece of (43). Hence, defining the variable $\mathcal{K} = z_m/z_0$ and then expanding (43) for large $\mathcal{K}$ one obtains,

$$\text{Length}(\gamma) \approx 2L\left(\log\frac{4z_0}{\epsilon} - \log\left[\frac{2}{\mathcal{K}} - \alpha + 2\sqrt{\beta}\right]\right) = \qquad (44)$$

$$= 2L\left(\log\frac{\xi}{\epsilon} + \log\frac{\mathcal{K}}{1-\widetilde{\lambda}\,\mathcal{K}}\right) ,$$

where,

$$\widetilde{\lambda} = \frac{1}{2}\left(\alpha - 2\sqrt{\beta}\right) = \frac{1}{2}\left[(q_1+q_2) - 2\sqrt{q_1\, q_2}\,\right] , \qquad (45)$$

$\xi = 2\,z_0$ and $\widetilde{\lambda}\,\mathcal{K} < 1$. It is importatant to note that $\widetilde{\lambda} > 0$ for any selection holding simulaneously that $q_1 \geq 1$, $q_2 > 1$ and $f(z_0) = 0$.

In equation (44) one finds two very different kind of terms: first there is an UV-dependent (ϵ-dependent) logarithmic term that is responsible for the *area law* of the entanglement entropy when applying (20). In addition, there is also an IR term $\log(\mathcal{K}/(1-\widetilde{\lambda}\,\mathcal{K}))$ which is quite a generic feature of holographic models with a gapped spectrum provided the growth of minimal surfaces at the IR region (see figure 7 lower part left). It is pertinent to note here that, if one reduces the size of the subsystem A (i.e, making ℓ smaller), eventually, the curve γ separates from the the tip of the soliton geometry at $z = z_0$ and the smaller size of A, now probes more directly, the UV region of the boundary field theory [32]. When this occurs, the IR term disappears.

As in the case of the non extremal soliton, it is possible to interpret the entangling nature of the IR fixed point shown by the large $\mathcal{K}$-ℓ expansion of Length(γ), in the language of the hybrid MPS-MERA tensor network state described in section II C. Once again, a tensor network composed of a MERA *curtain* of $\tau_0 = \log\xi$ layers with $\xi = 2\,z_0$ is considered. However, on the top of the MERA *curtain*, now lies an MPS state $|\psi_{MPS}\rangle$ with bond dimension $\mathcal{M} > 1$ that corresponds to a non trivial entangled state.

A similar argument to the case of the non-extremal soliton for the entanglement entropy of a region A with $\ell \gg \xi$, shows that the MERA *curtain* contribution to entanglement entropy is given by $S_A^{MERA} \propto \log\xi \sim S_0$. Nevertheless, in this case, the state $|\psi_{MPS}\rangle$ at the top of the network, provides an additional contribution S_A^{MPS} to the entanglement entropy of A. This non zero contribution results bounded by $\log\mathcal{M}$ (see eq.(9)) and the total entanglement entropy now amounts to,

$$S_A = S_A^{MERA} + S_A^{MPS} \leq \log\xi + 2\,\log\mathcal{M}\ . \tag{46}$$

As the entanglement collection on the top layer now yiels a non-zero result, it is reasonable to interpret that the curve $\widetilde{\gamma}_A$ acting as the boundary of the causal cone of A, has an IR flat bend-over region near the MERA *curtain* top layer. This is also consistent with the growth of minimal surfaces at the capping region in holographic models with a gapped spectrum. It is thus precisely S_A^{MPS}, the term which may be identified with the IR contribution to the geodesic length in (44) as far as it holds that,

$$\log\frac{\mathcal{K}}{1-\widetilde{\lambda}\,\mathcal{K}} \leq 2\,\log\mathcal{M}\ . \tag{47}$$

The two point function of two scaling operators $\Phi(-\ell/2)$ and $\Phi(\ell/2)$ located at the bottom of the tensor network, $\mathfrak{C}^{\ell}_{\text{TNS}} = \langle\Psi|\Phi(-\ell/2)\,\Phi(\ell/2)|\Psi\rangle$ can also be derived from simple arguments. Once again, $\tau_0 = \log\xi$ MERA contractions are carried out in order to obtain that,

$$\begin{aligned}
&\langle\Psi|\Phi(-\ell/2)\,\Phi(\ell/2)|\Psi\rangle = \\
&= \langle\psi_{MPS}|\,(\mathcal{S}(\Phi(-\ell/2))^{\tau_0}\,(\mathcal{S}(\Phi(\ell/2))^{\tau_0}\,|\psi_{MPS}\rangle = \\
&= (\mu)^{2\tau_0}\langle\psi_{MPS}|\Phi(-\ell/2\xi)\,\Phi(\ell/2\xi)|\psi_{MPS}\rangle\ .
\end{aligned} \tag{48}$$

Recalling that $\Delta \equiv -\log\mu$, and (8) one easily finds that,

$$\begin{aligned}
&\langle\Psi|\Phi(-\ell/2)\,\Phi(\ell/2)|\Psi\rangle = \\
&= \xi^{-2\Delta}\,\langle\psi_{MPS}|\Phi(-\ell/2\xi)\,\Phi(\ell/2\xi)|\psi_{MPS}\rangle = \\
&= \xi^{-2\Delta}\sum_{|\lambda_\nu|<1} c_\nu\,(\lambda_\nu)^{\ell/\xi}\ .
\end{aligned} \tag{49}$$

Here it will be assumed that the sum in (49), may be approximated by the term with the highest λ_ν i.e,

$$\mathfrak{C}^{\ell}_{\text{TNS}} = \langle\Psi|\Phi(-\ell/2)\,\Phi(\ell/2)|\Psi\rangle \approx \xi^{-2\Delta}\,c_2\,(\lambda_2)^{\ell/\xi}\ . \tag{50}$$

As in previous sections, it is interesting to compare this result with the two point function of two scaling operators of the boundary theory separated a distance ℓ, when it is obtained through (44) and the holographic prescription (29, 30). Proceeding in this way, one finds that,

$$\begin{aligned}
&\mathfrak{C}^{[\ell]}_{\text{Holog}} = \epsilon^{-2\Delta}\,e^{-m\,\text{Length}(\gamma)} = \\
&= \epsilon^{-2\Delta}\,e^{-2\Delta\left(\log\xi/\epsilon + \log\mathcal{K}/(1-\widetilde{\lambda}\,\mathcal{K})\right)} = \\
&= \xi^{-2\Delta}\left(\frac{1-\widetilde{\lambda}\,\mathcal{K}}{\mathcal{K}}\right)^{2\,\Delta}\ .
\end{aligned} \tag{51}$$

By a direct comparison between (50) and (51), one realizes how similar are the *holographic* structure of the two point functions offered from MERA-like tensor networks and the AdS/CFT. It is thus tempting to further identitfy some relevant parameters defining both approaches. Assuming that the order of the scaling dimension of operators Φ are $\mathcal{O}(\Delta) \sim 1$, it is thus possible to identify the exponentially decaying terms $(\lambda_2)^{\mathcal{K}}$ and $((1-\widetilde{\lambda}\,\mathcal{K})/\mathcal{K})^{2\,\Delta}$

in (50) and (51) respectively, which yields,

$$\log \frac{\mathcal{K}}{1-\widetilde{\lambda}\,\mathcal{K}} \sim -\frac{\mathcal{K}}{2}\,\log \lambda_2 = \eta\,\mathcal{K}\ , \tag{52}$$

with

$$\eta = -\frac{1}{2}\,\log \lambda_2\ . \tag{53}$$

As a result, equation (44) may be expressed as,

$$\mathrm{Length}(\gamma) \approx 2L\,\left(\log \frac{\xi}{\epsilon} + \eta\,\mathcal{K}\right)\ . \tag{54}$$

The *extensive* term $\eta\,\mathcal{K}$ is consistent with the fact that, in general, any holographic geometry that is capped is a candidate for showing extensive behaviour provided the growth of the minimal surface γ when it bends over the infrared region. The identification of the exponentially decaying terms posed in (52) may be pushed even further in order to obtain a direct relationship between parameters of the tensor network and parameters of the holographic geometry. Indeed, considering the limit $\eta\,\mathcal{K} \ll 1$ in (52) one finds that,

$$\eta = -\frac{1}{2}\,\log \lambda_2 \sim \frac{\log \mathcal{K}}{\mathcal{K}} + \widetilde{\lambda}\ , \tag{55}$$

and

$$\eta|_{\mathcal{K}\to\infty} \sim \lim_{\mathcal{K}\to\infty} \frac{\log \mathcal{K}}{\mathcal{K}} + \widetilde{\lambda} = \lim_{\mathcal{K}\to\infty} \frac{1}{\mathcal{K}} + \widetilde{\lambda} = \widetilde{\lambda}\ . \tag{56}$$

As a result, one may conclude that the AdS/MERA duality provides a relationship between the parameter $\widetilde{\lambda}$ defining the extremal AdS soliton geometry and the eigenvalue λ_2 of the identity transfer matrix corresponding to the top MPS tensor. This connection can be written as,

$$\widetilde{\lambda} \sim -\frac{1}{2}\,\log \lambda_2\ . \tag{57}$$

It is worthy to notice here that, all the identifications and conclusions raised from (44) are only valid when $\widetilde{\lambda} > 0$. For the extremal soliton defined by $q_1 = q_2 = 1$, the parameter $\widetilde{\lambda}$ is zero. Applying $\widetilde{\lambda} = 0$ to (54) one obtains that,

$$\mathrm{Length}(\gamma) \approx 2L\,\log \frac{\xi}{\epsilon}\ . \tag{58}$$

This result for the geodesic length corresponds to a a non-extremal soliton, which obviously is a wrong conclusion because $\widetilde{\lambda} = 0$ was applied where not allowed. Instead, when considering $\widetilde{\lambda} = 0$ in equation (44), one obtains,

$$\text{Length}(\gamma) = 2L \left(\log \frac{\xi}{\epsilon} + \log \mathcal{K} \right) = 2L \, \log \frac{\ell}{\epsilon} \, , \tag{59}$$

which corresponds to the geodesic length in pure AdS_3 or in AdS/MERA terms, to a pure scale invariant MERA tensor network.

V. DISCUSSION AND CONCLUDING REMARKS

By exploring some hints posed in [16], it has been explicitly shown that the entanglement entropy and the two point correlators in a type of hybrid tensor network state composed by a finite number of MERA layers and an MPS acting as a cap layer, resemble the behaviour of the holographic entanglement entropy and the holographic two point functions appearing in the AdS soliton geometries. Within the context of the AdS/CFT correspondence, the AdS soliton is a capped geometry representing a theory with a mass gap. It was thus expected that the entanglement at the IR point would be zero when considering models where no *topological order* is present. This is the case of the non extremal soliton, in which, by making use of the holographic formula for the entanglement entropy, no hints of long range entanglement were found. According to this, a tensor network representation of the non extremal soliton which is characterized by an MPS cap tensor that is a trivial product state has been proposed. At variance, for extremal soliton geometries, the holographic formula for the entanglement entropy leads to find nontrivial behaviours for the long range entanglement, which might be related to some underlying topological order [16]. In this case, the capping tensor in the dual tensor network results in a non trivially entangled matrix product state with finite, non zero bond dimension.

Assuming the striking relationship between MERA and AdS/CFT, a connection between some parameters of the tensor network represenation and those parameters which define the holographic geometry of an AdS soliton is provided. Indeed, equation (57) relates the spectrum of the tranfer matrices of the cap MPS tensor with the parameters q_1 and q_2 defining the soliton in AdS. This kind of result may be useful in order to, *via* AdS/MERA, open the possibility to classify the gapped phases of 1D-quantum many-body systems in terms of their associated geometry. As posed in [34], different topological phases of 1D gapped systems with an MPS representation, can be characterized by the spectrum of the MPS tranfer matrices.

The proposal in this paper could be extendable to higher dimensions. Namely, there are 2D generalizations of MERA [35] and MPS (PEPS) [6] to reasonably construct 2D versions of the hybrid network proposed here. In [36], authors presented the MERA tensor network for the Kitaev's toric code model [37], a topologically ordered phase in two spatial dimensions. The MERA tensor network for the toric code model is capped off by a top tensor which encodes the information about the topological order. Furthermore, and in a closer analogy to the tensor networks considered here, the toric code also possess a very simple representation in terms of a PEPS with a bond dimension $\mathcal{M} = 2$ [38]. Indeed, for any PEPS with a finite bond dimension, it is always simple to calculate the topological entanglement entropy defined in [39].

Finally, in [40], authors provide the gravity dual of a (2+1) dimensional field theory which in its IR limit flows to a pure Chern-Simons theory. Since the theory is gapped, the geometry is capped off at IR. To complete the model, D7-branes are located on the tip of the cigar-like soliton geometry, making the IR behavior different from that of the "naked" AdS soliton geometry. Concretly, from the D7-branes arises a Chern-Simons term, which gives rise to a topological entanglement entropy term through (19). It is thus tempting to apply the ideas presented here in the context of higher dimensional geometries i.e, finding 2D tensor network states with top tensors whose entanglement properties match those observed in the geometric duals of [40].

Acknowledgments

JMV is grateful to P. Sodano, J. Prior, S. Montangero, L. Tagliacozzo and G. Sierra for very fruitful insights at different stages of this project. JMV has been supported by the Spanish Office for Science FIS2009-13483-C02-02 and Fundación Séneca Región de Murcia 11920/PI/09. I thank the Centro de Ciencias de Benasque Pedro Pascual (Spain) and the International Institute of Physics in Natal (Brazil) for their hospitality at several stages of

this project.

---

[1] O. Aharony, S. S. Gubser, J.M Maldacena, H. Ooguri and Y. Oz, Large N Field Theories, String Theory and Gravity, Phys. Rept. 323 (2000) 183 [hep-th/9905111]; J. M. Maldecena, The Large N Limit of Superconformal Field Theories and Supergravity, Adv. Theor. Math. Phys. 2 (1998) 231 [hep-th/9711200]; S. S. Gubser, I. R. Klebanov, and A. M. Polyakov, Gauge Theory Correlators from Non-Critical String Theory, Phys. Lett. B 428 (1998) 105 [hep-th/9802109]; E. Witten, Anti-de Sitter Space, Thermal Phase Transition, And Confinement In Gauge Theories, Adv. Theor. Math. Phys. 2 (1998) 505 [hep-th/9803131].

[2] M. R. Douglas, L. Mazzucato and S. S. Razamat, Holographic dual of free field theory, Phys.Rev.D 83 (2011) 071701, [arXiv:1011.4926 [hep-th]]

[3] J. de Boer, E. Verlinde and H. Verlinde, On the Holographic Renormalization Group, JHEP 0008 (2000) 003 [hep-th/9912012]; M. Fukuma, S. Matsuura and T. Sakai, Holographic Renormalization Group, Prog.Theor.Phys. 109, 489-562 (2003) [hep-th/0212314].

[4] S. R. White, Density matrix formulation for quantum renormalization groups, Phys. Rev. Lett. 69, (1992) 2863.

[5] D. Perez-Garcia, F. Verstraete, M.M. Wolf and J.I. Cirac, Matrix Product State Representations, Quantum Inf. Comput. 7, (2007) 401 [quant-ph/0608197].

[6] F. Verstraete, J.I. Cirac, V. Murg, Matrix Product States, Projected Entangled Pair States, and variational renormalization group methods for quantum spin systems, Adv. Phys. 57, (2008) 143 [arXiv:0907.2796 [quant-ph]]

[7] M. Levin and C.P. Nave, Tensor renormalization group approach to 2D classical lattice models, Phys. Rev. Lett. 99, (2007) 120601 [cond-mat/0611687 [cond-mat.stat-mech]].

[8] Z. Gu and X.-G Wen, Tensor-entanglement-filtering renormalization approach and symmetry-protected topological order, Phys. Rev. B. 80, 155131 (2009) [arXiv:0903.1069 [cond-mat.str-el]].

[9] G. Vidal, Entanglement Renormalization, Phys. Rev. Lett. 99, (2007) 220405 [cond-mat/0512165 [cond-mat.str-el]]

[10] B. Swingle, Entanglement Renormalization and Holography, Phys. Rev. D 86, (2012) 065007, [arXiv:0905.1317v1 [cond-mat.str-el]].

[11] G. Evenbly and G, Vidal, Tensor network states and geometry, J Stat.Phys. 145, (2011) 891-918, [arXiv: 1106.1082v1 [quant-ph]].

[12] M. Van Raamsdonk, Comments on quantum gravity and entanglement, [arXiv:0907.2939 [hep-th]]; Building up spacetime with quantum entanglement, Gen.Rel Grav. 42, (2010) 2323; Int. J. Mod. Phys. D 19 (2010) 2429 [arXiv:1005.3035 [hep-th]].

[13] J. Molina-Vilaplana and P. Sodano, Holographic View on Quantum Correlations and Mutual Information between Disjoint Blocks of a Quantum Critical System, JHEP. 10 (2011) 011 [arXiv:1108.1277 [quant-ph]]; J. Molina-Vilaplana, Connecting Entanglement Renormalization and Gauge/Gravity dualities, [arXiv:1109.5592 [quant-ph]].

[14] V. Balasubramanian, M. B. McDermott and M. Van Raamsdonk, Momentum-space entanglement and renormalization in quantum field theory, [arXiv:1108.3568 [hep-th]].

[15] H. Matsueda, Scaling of entanglement entropy and hyperbolic geometry, [arXiv:1112.5566 [cond-mat.stat-mech]].

[16] M. Ishihara, F. -L. Lin and B. Ning, Refined Holographic Entanglement Entropy for the AdS Solitons and AdS black Holes, [arXiv:1203.6153 [hep-th]].

[17] H. Matsueda, M. Ishihara and Y. Hashizume, Tensor Network and Black Hole, [arXiv:1208.0206 [hep-th]].

[18] K. Okunishi, Wilson's numerical renormalization group and AdS_3 geometry, [arXiv:1208.1645 [hep-th]].

[19] H. Matsueda, Multiscale Entanglement Renormalization Ansatz for Kondo Problem, [arXiv:1208.2872 [cond-mat.stat-mech]].

[20] M. Nozaki, S. Ryu and T. Takayanagi, Holographic Geometry of Entanglement Renormalization in Quantum Field Theories, [arXiv:1208.3469 [hep-th]].

[21] J. Haegeman, T. J. Osborne, H. Verschelde and F. Verstraete, Entanglement renormalization for quantum fields, [arXiv:1102.5524 [hep-th]].

[22] B. Swingle, Constructing holographic spacetimes using entanglement renormalization, [arXiv:1209.3304 [hep-th]].

[23] S. Ryu and T. Takayanagi, Holographic Derivation of Entanglement Entropy from the antide Sitter Space/Conformal Field Theory Correspondence, Phys. Rev. Lett. 96, (2006) 181602 [hep-th/0603001]; Aspects of Holographic Entanglement Entropy, JHEP 0608 (2006) 045 [hep-th/0605073]; T. Nishioka, S. Ryu, and T. Takayanagi, J.Phys.A 42(2009) 504008

[arXiv:0905.0932 [hep-th]]; T. Takayanagi, Entanglement Entropy from a Holographic Viewpoint, Class. Quantum Grav, 29, 153001 (2012) 153001 [arXiv:1204.2450 [gr-qc]].

[24] U. Schollwoeck, The density-matrix renormalization group in the age of matrix product states Ann of Phys. 326, (2011) 96 [arXiv:1008.3477 [cond-mat.str-el]].

[25] M. Rizzi, S. Montangero, P.Silvi, V. Giovanetti and R. Fazio, Homogeneous multiscale entanglement renormalization ansatz tensor networks for quantum critical systems, New J. Phys, 12, (2010) 075018.

[26] R. N. C.Pfeifer, G. Evenbly and G. Vidal, Entanglement renormalization, scale invariance, and quantum criticality, Phys. Rev. A. 79 (4), (2009) 040301(R) [arXiv:0810.0580 [cond-mat.str-el]].

[27] F. Pollmann, E. Berg, A. M. Turner, and M. Oshikawa, Symmetry protection of topological phases in one-dimensional quantum spin systems, Phys.Rev.B, 85, (2012) 075125 [arXiv:0909.4059 [cond-mat.str-el]].

[28] M. Headrick and T. Takayanagi, A holographic proof of the strong subadditivity of entanglement entropy, Phys. Rev. D 76 (2007) 106013, [arXiv:0704.3719 [hep-th]].

[29] H. Casini, M. Huerta and R. C. Myers, Towards a derivation of holographic entanglement entropy, JHEP 1105 (2011) 036, [arXiv:1102.0440 [hep-th]]; R. C. Myers and A. Sinha, Holographic c-theorems in arbitrary dimensions, JHEP 1101 (2011) 125, [arXiv:1011.5819 [hep-th]].

[30] J.D. Brown and M. Henneaux, Central charges in the canonical realization of asymptotic symmetries: an example from three-dimensional gravity, Comm. Math.Phys, 104, (1986) 207-226.

[31] J.L.F. Barbón, C.A. Fuertes, Holographic entanglement entropy probes (non)locality, JHEP 0804, (2008) 096 [arXiv:0803.1928 [hep-th]].

[32] I.R, Klebanov, D. Kutasov, and A. Murugan, Entanglement as a Probe of Confinement, Nucl. Phys B, 796, 274 (2008) [arXiv:0709.2140 [hep-th]].

[33] P. Calabrese and J. Cardy, Entanglement Entropy and Quantum Field Theory, J. Stat. Mech, 0406, (2004) P06002 [hep-th/0405152].

[34] F. Pollman and A. Turner, Detection of Symmetry Protected Topological Phases in 1D, Phys. Rev. B,86, (2012) 12544 [arXiv:1204.0704]

[35] G. Evenbly and G. Vidal, Entanglement renormalization in two spatial dimensions, Phys.Rev.Lett, 102, (2009) 180406, [arXiv:0811.0879 [cond-mat.str-el]].

[36] M. Aguado and G. Vidal, Entanglement renormalization and topological order, Phys. Rev. Lett. 100, (2008) 070404, [arXiv:0712.0348 [cond-mat]].

[37] A. Y. Kitaev, Fault-tolerant quantum computation by anyons, Ann. Phys. 303, (2003) 2, [quant-ph/9707021].

[38] F. Verstraete, M.M. Wolf, D. Perez-Garcia, J.I. Cirac, Phys.Rev.Lett. **96**, 220601, (2006); [arXiv:0601075 [quant-ph]].

[39] A. Y. Kitaev and J. Preskill, Topological entanglement entropy, Phys.Rev.Lett. 96, (2006) 110404,, [arXiv:0510092 [hep-th]].

[40] M. Fujita, W. Li, S. Ryu, T. Takayanagi, Fractional Quantum Hall Effect via Holography: Chern-Simons, Edge States, and Hierarchy, JHEP 0906, (2009) 066, , [arXiv:0901.0924 [hep-th]].

[41] A superoperator is a linear operator acting on a linear space of linear operators. The prefix super- have no connection to supersymmetry or superalgebras